Available online at www.sciencedirect.com
SCIENCE DIRECT®
Journal of Applied Geophysics 54 (2003) 127–144
JOURNAL OF APPLIED GEOPHYSICS
www.elsevier.com/locate/jappgeo

4-D ground penetrating radar monitoring of a hydrocarbon leakage site in Fortaleza (Brazil) during its remediation process: a case history

David Lopes de Castro*, Raimundo Mariano Gomes Castelo Branco

Laboratório de Geofísica-Departamento de Geologia, Universidade Federal do Ceará Campus Universitário do Pici, Bloco 913 60455-760, Fortaleza-CE, Brazil

Received 25 October 2002; accepted 29 August 2003

Abstract

A 4-D monitoring GPR survey was carried out in order to outline the light non-aqueous phase liquid (LNAPL) plume underground during a remediation process in the area of an impacted gas station in Fortaleza, NE Brazil. The complex GPR signature of the plume was well characterized. Low reflectivity zone corresponds to hydrocarbon vapor phase in the vadose zone. Enhanced reflections are associated with free and residual products directly above the water table. A theoretical model based on geochemical zonation of the LNAPL was calculated using a finite difference time domain (FDTD) forward modeling code, whose synthetic radargrams provide useful insight into the nature of the reflection events related to LNAPL contamination. Hydrogeologic and hydrochemical data from installed monitoring wells provided additional support for interpreting of the GPR response. Moreover, a network of radar sections collected during fifteen months at the polluted site show clearly temporal changes in the plume dimensions, induced by regular pumping of groundwater. This corrective action caused an important drop of the water table that was followed by a rapid shrinking of the impacted area in the vadose zone, generating pooling of vapor products. A steady restore of the reflectivity in the shadow zone suggests a decrease of LNAPL saturation along the GPR survey.

Keywords: Ground penetrating radar; Hydrocarbon leakage; 4-D survey; Forward modeling

1. Introduction

Leaks of hydrocarbon products from underground storage tanks (UST) are generally of concern to public safety. The occurrence of organic compounds in water can create a hazard to public health and the environment. Because the seriousness of this environmental problem, their detection in the subsurface using geophysical methods, particularly Ground Penetrating Radar (GPR), has been the subject of considerable interest among geophysicists in the last decades.

The primary physical properties of organic contaminants, such as light non-aqueous phase liquids (LNAPL) and dense non-aqueous phase liquids (DNAPL), that may be detectable using geophysical

* Corresponding author. Fax: +55-2185-288-9874.
E-mail addresses: david@ufc.br (D. Lopes de Castro), mariano@ufc.br (R.M.G.C. Branco).

0926-9851/$ - see front matter © 2003 Elsevier B.V. All rights reserved.
doi:10.1016/j.jappgeo.2003.08.021

methods are the electrical parameters of conductivity and permittivity (Daniels et al., 1995). Hydrocarbons typically have higher apparent resistivity (Asquith and Gibson, 1982) and lower relative permittivity than background waters. However, hydrocarbon plumes may also be delineated as resistivity lows if inorganic compounds are added to contaminated groundwater to stimulate bioremediation, thus increasing the total dissolved solids (TDS) in the water (Benson et al., 1997). TDS content can also be increased in groundwater, which associated with the biodegradation of the hydrocarbon plume. Consequently, TDS can promote an enhancement of the apparent conductivity.

Nevertheless, NAPL contamination has a more complex geophysical signature because the typical hydrocarbon spill in the subsurface differentiates into various components. Gaseous and residual zones develop above the water table, and the product core, an immiscible phase, is located between the capillary fringe and water table, with a diffuse mixing region below. In the saturated zone, a partially dissolved phase mixed with air and water can migrate, following the local hydrologic gradient. The distribution and migration of the underground fluids (NAPL) is very complex and depends on the physical characteristics of the original regolith, the nature and quantity of the contaminant, hydrogeologic conditions, rainfall, and the seasonal variations of the water table level. Daniels et al. (1995) provide a summary of hydrocarbon behavior in depth, as well as its physical properties.

In many cases, GPR is the more adequate geophysical tool for detecting contaminated areas. GPR signal provides a high resolution imaging of plume components, especially in the vadose zone above the water table, even in intensive occupied urban areas, where background electromagnetic noise strongly limits the application of other electrical and electromagnetic methods. Therefore, since the 1980s, extensive field and laboratory studies have been conducted to investigate the geophysical response to hydrocarbon contaminants in earth materials. Olhoeft (1986) and Daniels et al. (1992) conducted studies on the detectability of non-aqueous fluid with high frequency electromagnetic techniques, which has been based primarily upon the relative permittivity of the material. Redman et al. (1994) described a decrease in the GPR reflection amplitude at the water table in areas impacted by kerosene. Daniels et al. (1995) attributed to the vapor phase of the gasoline displacing water a zone of diminished reflections from sedimentary features above the hydrocarbon floating in the vadose zone. On the other hand, Campbell et al. (1996) report an enhanced, higher amplitude saturated zone reflection under the spill, in controlled spill experiments. Probably, the LNAPL displaces the water from the transition zone above the capillary fringe, thus making a sharp interface at the water table.

In addition, Sauck (2000) proposes a geoelectrical model for LNAPL plumes and their environs in sandy sediments. The contaminated area can be divided into six general zones with respect to geochemical behavior in the vadose and saturated zones, as described in Table 1. This model will be took into account and discussed by the GPR analysis.

In 2000, the notification of a hydrocarbon leakage from UST at a gasoline station in Fortaleza, a 2 million people city in NE Brazil, gave the Laboratory of Geophysics of Ceará Federal University the opportunity of contaminant plume characterization based on GPR, hydrogeologic and hydrochemical data. A commercial remediation procedure was put into effect in December 2000 to reduce underground contamination. During 15 months, contaminant plume changes, which were caused by corrective action and seasonal variations, were documented in several GPR surveys. The qualitative analysis and forward modeling of these detailed data presented

Table 1
Geoelectrical model for the LNAPL of Sauck (2000)

Zone	Location	Hydrocarbon product
1	Vadose zone directly beneath the spill	Residual and Vapor phases
2	Vadose zone directly above the water	Free (mobile) and Residual phases
3	Vadose zone directly above the free/residual product	Vapor and Residual phases
4	Reactive fringe around the dissolved plume	Dissolved phase
5	Anaerobic core of the dissolved plume	Dissolved phase
6	Distal end of the dissolved plume	Dissolved phase

here represent an interesting and thorough case history, whose results could be useful to understand complex and dynamic evolution of LNAPL plumes at depth.

Another interesting aspect of this study is that the gasoline sold in Brazil comprises a mixture of 76% of gasoline and 24% of ethanol. Corseuil et al. (2000) investigated the effects ethanol-amended gasoline may cause on aquifers in spill sites. They concluded that ethanol can persist in the aquifer for long periods and interfere in the biodegradation of the more toxic organic compounds, impeding, or at least retarding, natural hydrocarbon degradation in groundwater. The contribution of the ethanol-amended gasoline to electromagnetic response of the contaminant plume has been rarely reported and is evaluated in this study using GPR data.

2. Site overview

The study site is located in a densely part of the city, which is occupied by both residential and commercial buildings, including the campus of the Ceará Federal University. Since 2000, the state company of urban traffic has been constructing a subway line at Carapinima Avenue (Fig. 1). The detection of the gasoline leakage from an underground storage tank of the gas station occurred during excavation in the second semester of 2000.

According to Brandão (1995), the coastal plain of Fortaleza is composed of Precambrian crystalline rocks, which are overlain by Late Tertiary sedimentary rocks (Barreiras Formation). This sedimentary cover is overlain by Quaternary alluvial and aeolian (paleodunes) sediments. The shallow underground geology of the study site consists of unconsolidated to semiconsolidated alluvial and aeolian deposits of gravel, sand, silt and clay. The soil stratigraphy was described during the removal of leaking UST (Fig. 2). Its analysis was also based on soil samples from monitoring wells. The upper soil unit is 0.5 m thick and consists of a very fine to fine yellowish sand. An intermediary soil layer is composed of fine to medium aeolian massive to finely laminated sand. The contaminant plume developed mostly in this layer, whose geologic properties, e.g. good textural homogeneity and low clay content, guaranteed a good hydrologic conductivity. In the contaminated zone, the sand impregnated with gasoline showed a dark color and formed small nodules. The contact of the intermediate layer and a lower silty–clay soil unit, which is 4.5–5.0 m deep, is gradational.

The study site is located in an almost horizontal area, with less than 1 m of difference in elevation across the site. The climate is typical from equatorial regions, with two well-marked seasons: one dry from June to February; and one humid between March and May. Before the beginning of the remediation process, the water table depths in monitoring wells at the gas station were up to 2.35 m. A slight gradient indicated a flow direction to southwest in agreement with regional topography.

3. Leakage and remediation

The first register of a leak from an UST of the gas station was reported in 1998. Gasoline contaminated the groundwater that was pumped from a drinking well of the neighboring residential building (Fig. 1). To solve this problem, the gas station owner constructed a new well in the neighboring ground, far away from the leaking UST. At that time, no corrective action was carried out to remediate the leakage. Afterwards, the contaminated well was definitively abandoned. Eventually in 2000, during the excavation of the subway at Carapinima Avenue, gasoline contamination was detected both in soil and groundwater. Finally, a remediation process was initiated at the impacted area.

First, new glass fiber tanks were installed at the station in January and February 2001, in order to replace those of metallic nature. Two months after the replacement, the old leaking tanks were removed, revealing a seriously contaminated site (Fig. 2). Five pumping wells and 12 monitoring wells were distributed in the gas station area in order to pump free product and contaminated water, to delineate the flow of groundwater, and to monitor the progress of the remediation efforts. Since April 2001, groundwater has been pumped regularly and has being treated on the site to remove contaminants. This action has directly caused an overall drop of the water table about 4 m around the impacted area. GPR surveys were conducted before the beginning of the remedi-

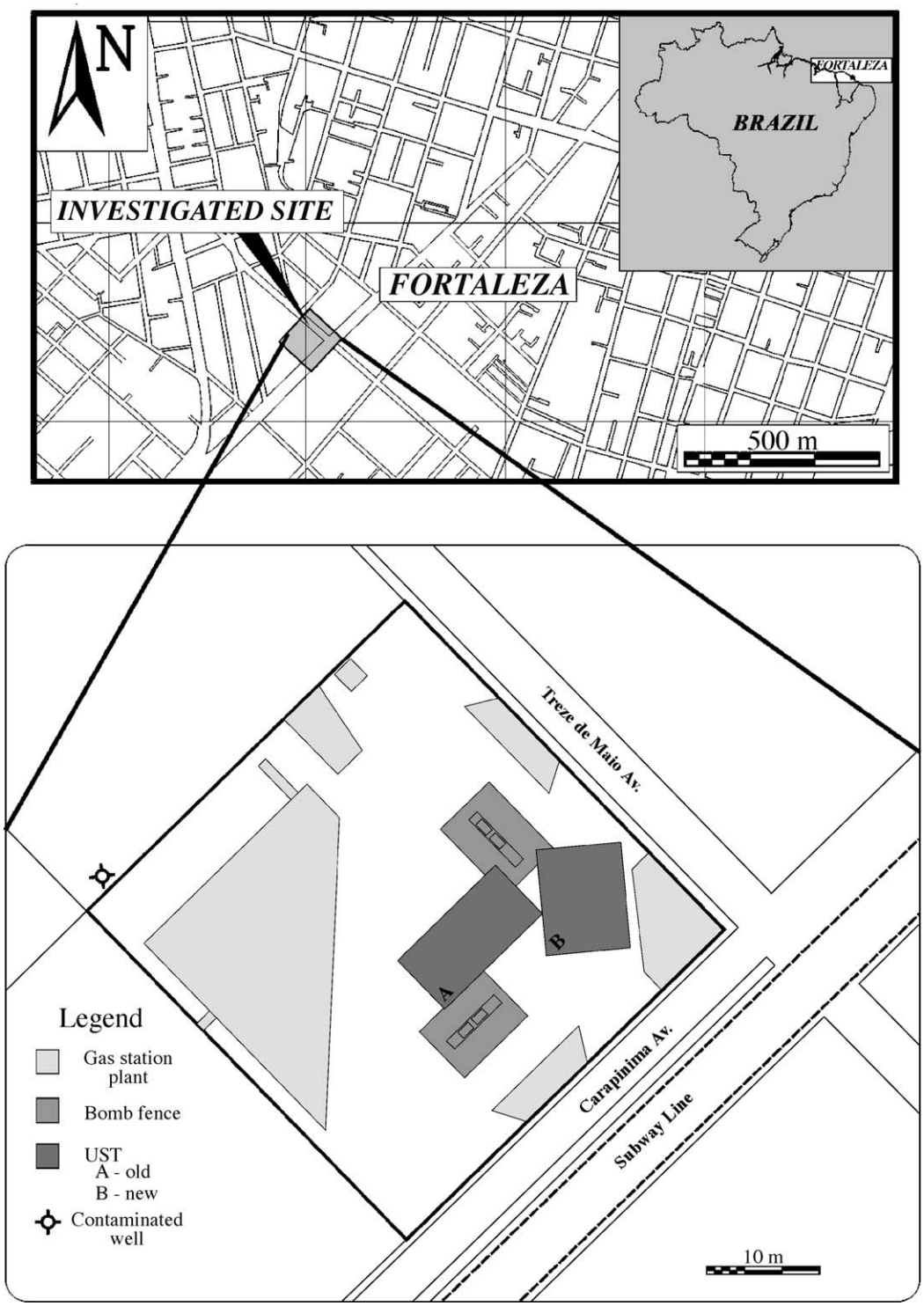

Fig. 1. Location map of the contaminated gasoline station in Fortaleza, Brazil. UST: underground storage tanks.

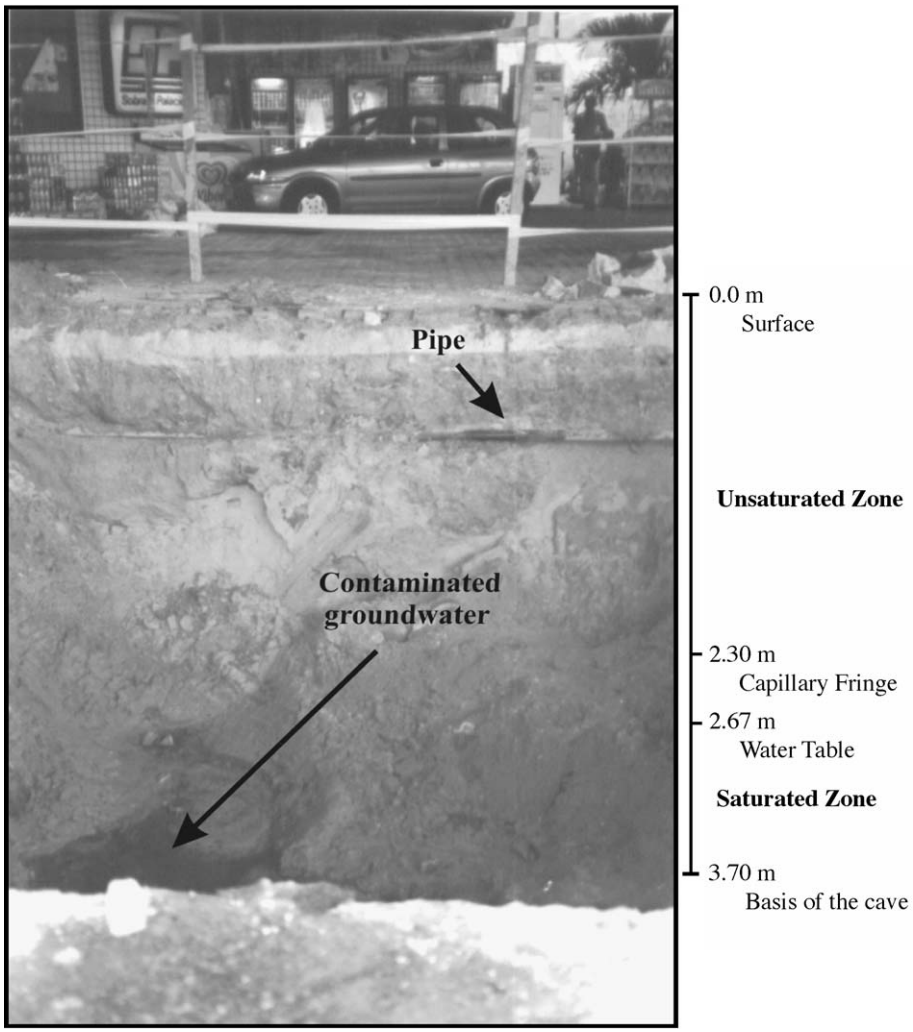

Fig. 2. The pulling of the leaking UST reveals a pool of free-floating LNAPL and allows a direct comparison between the underground geology and GPR signal.

ation action as well as during the well pumping along 1 year.

4. GPR data

Radar data were produced with a GSSI SIR-2000 system during nine surveys between January 2001 and March 2002. Up to 150 GPR lines were made at the study area, comprising about 4550 m of GPR profile. Fig. 3 shows the location of radar lines made during each survey. Two surveys were carried out in January and October 2001 to improve GPR response of the contaminant plume at the site. In this case, measurements were made with 900, 400, 200 and 80 MHz antennas. The other surveys were carried out with 400 and 200 MHz antennas to register the plume evolution during the remediation action, initiated in January 2001.

GSSI antennas with 900, 400 and 200 MHz center frequencies are monostatic and blinded, whereas the 80 MHz antennas are bistatic and present a fixed

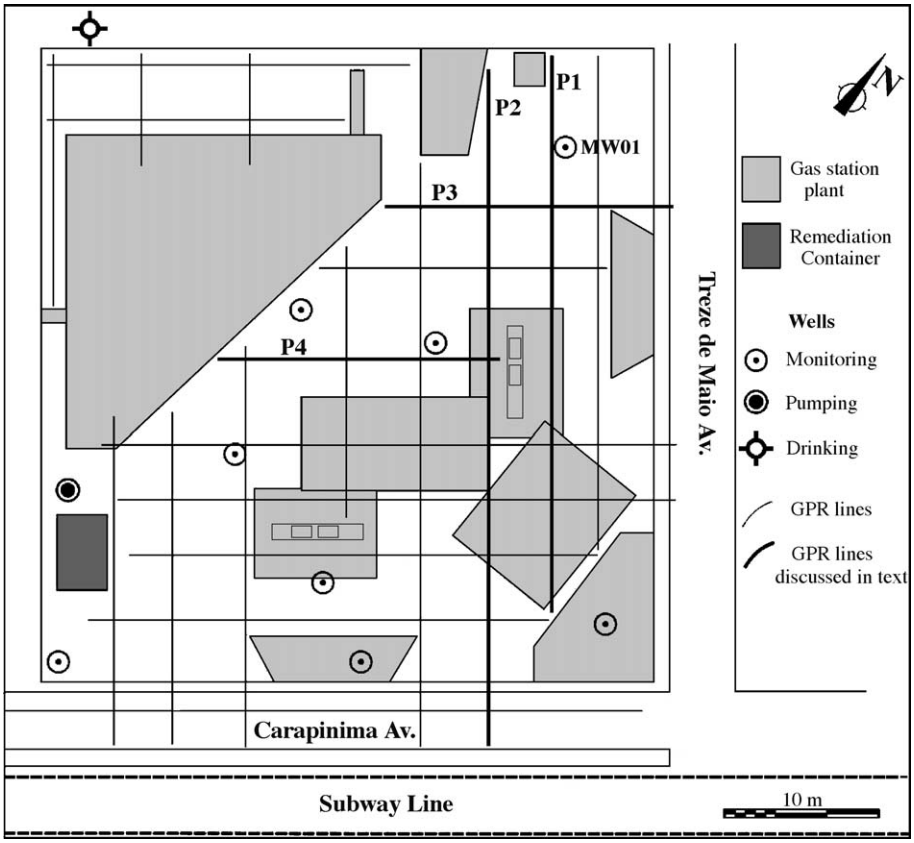

Fig. 3. GPR profile and well locations at the study site.

transmit-receiver separation of 1.0 m. Acquisition parameters were 512 sample/scan, 40 scans/m, three pole vertical Infinite Impulse Response (IIR) low pass filter between 1500 and 150 MHz, and three pole vertical IIR high pass filter between 150 and 15 MHz. Slight horizontal smoothing was done by applying a three scan moving average filter. A time varying gain (TVG) was automatically set to equalize amplitudes to 75% of full scale. Measurements were recorded in time windows between 15 and 250 nanoseconds (ns). In specific cases, post acquisition filtering was applied to improve a better signal to noise ratio. The radar data processing included FIR bandpass filters, 2D spatial filter and predictive deconvolution.

The depth of reflections on GPR sections was determined from the radar propagation velocity on the ground. This average velocity was calculated to be approximately 0.12 m/ns based on a comparison of GPR data with the water table measurements in monitoring wells, as well as directly in the cave during the removal of leaking tanks. The resulting average dielectric constant is up to 6.0, which is representative of clean, dry sand (Davis and Annan, 1989) and corresponds to the value obtained in a contaminated gas tank farm in Indiana by Daniels et al. (1995).

In order to estimate the average velocity more accurately, it was tried to fit the diffractions corresponding to the new tanks (see Fig. 4). However, the resulted velocities up to 0.29 m/ns certainly are not representative of the physical properties of the ground in the site. The broad aperture of the hyperboles seems to reflect the cylindrical geometry of the glass fiber tanks, what difficulties to determine the correct ground velocity by diffraction fit method.

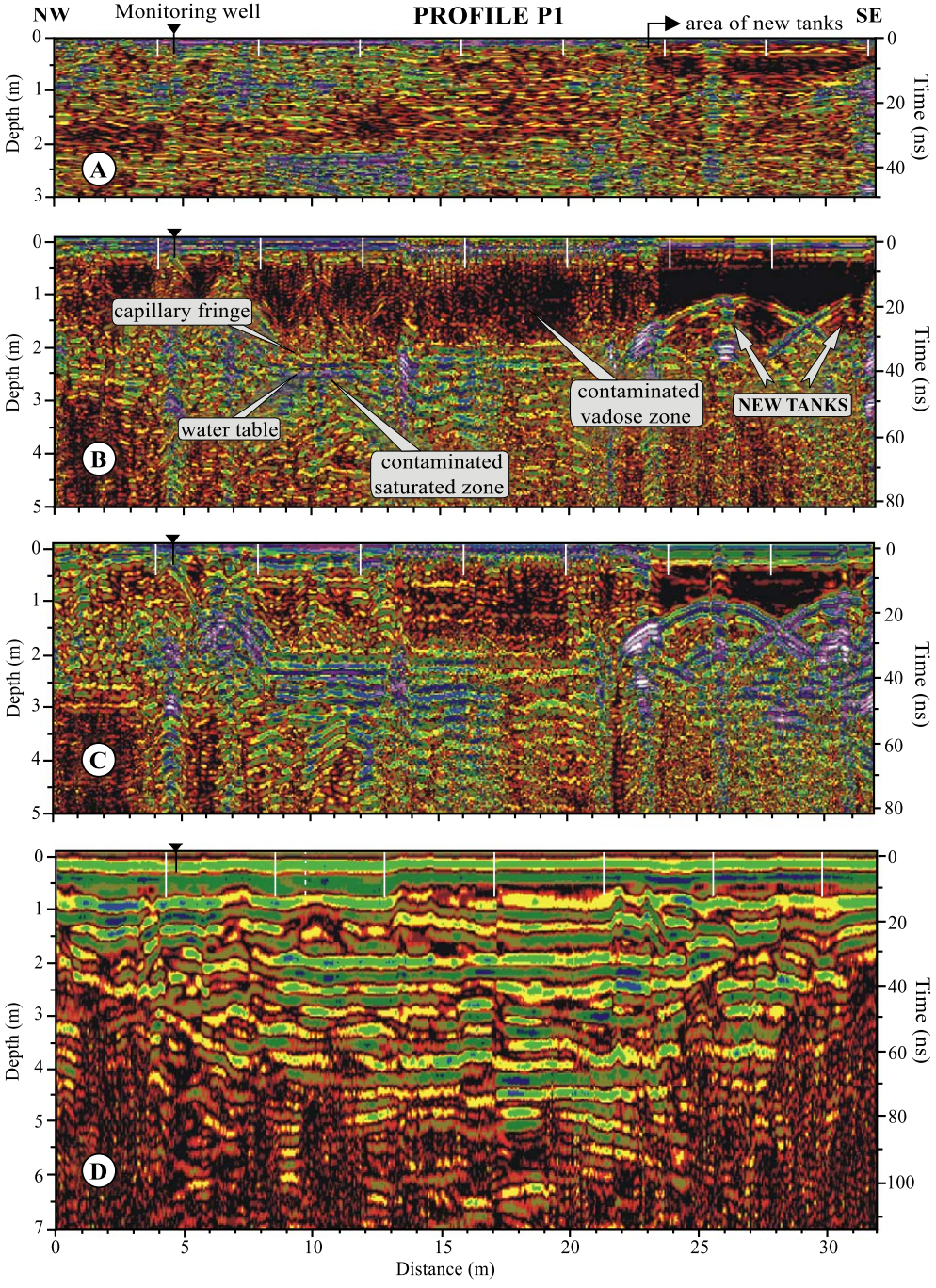

Fig. 4. GPR response of the contaminant plume for 900 (A), 400 (B), 200 (C) and 80 MHz (D) antennas at the gas station in Fortaleza, Brazil. Vertical scale exaggeration = 2.0.

5. GPR response of the hydrocarbon plume

The GPR data were collected using 900, 400, 200 and 80 MHz antennas in order to characterize the radar response of the contaminant plume at different center band frequencies. In this study, the better correlation between depth of investigation, given by lower frequencies antennas, and spatial resolution, given by higher frequencies antennas, was obtained with the 200 and 400 MHz antennas. The low-frequency (200 MHz) data provide a gross picture of the impacted sub-surface, while the higher-frequency (400 MHz) data provide a detailed picture of the near surface, principally in the vadose zone and transition zone above the water table. The 80 and 900 MHz data play a secondary role in the plume characterization in the site, due to either poor resolution signature of the near subsurface or shallow depth penetration free from noise, respectively.

GPR sections (Fig. 4) obtained with different antennas at profile P1 (Fig. 3) in October 2001 show a typical radar response of the contaminant plume at different antennas on the gas station. The acquisition and processing parameters of these sections are described at Table 2. A 2D spatial filter (200–1440 MHz) was applied to remove coherent ringing in the 900 MHz, which is present after 15 ns traveltime. As a result, the filtered section (Fig. 4A) is free from bands of ringing noise. However, the radar response of the contaminated zone is less obvious than in lower frequency data (Fig. 4B and C). To the 200 and 400 MHz data, just FIR bandpass filters (Table 2) were applied, due to the high record quality. Finally, a predicative deconvolution and a FIR bandpass (30–100 MHz) were applied to the 80 MHz data to increase the record resolution and to eliminate low and high frequencies noise, respectively.

Table 2
Acquisition parameters of the GPR sections depicted in Fig. 4

Center frequency (MHz)	Time window (ns)	Sampling (ns)	Post-acquisition filtering
900	50	0.1	2D Spatial Filter (200–1440 MHz)
400	85	0.14	FIR Bandpass (200–965 MHz)
200	85	0.2	FIR Bandpass (105–650 MHz)
80	115	0.39	Predictive deconvolution FIR Bandpass (30–100 MHz)

In the sections of Fig. 4, a region of attenuated reflections or shadow zone occurs in the vadose zone. This impacted zone is better seen between 10 and 22 m in the profile and up to 2.5 m depth (Fig. 4B and C). Fig. 5 shows an important lateral variation in the 400 MHz radar records at the near surface zone. The fence diagrams from profiles P2, P3 and P4 illustrate very well the difference between contaminated and uncontaminated areas in the gas station. The zone of attenuated GPR reflections can be spatially correlated with the area of known hydrocarbon contamination, as determined from soil probes at the old tanks cave and hydrochemical analysis.

According to Daniels et al. (1995), the low-amplitude reflection can be attributed to smaller plane wave reflection coefficients from the unsaturated sand, partially filled with vapor phase of LNAPL. The relative permittivity (k) decrease of the sand is probably due to the water ($k \approx 80$) in the unsaturated zone may have been displaced by gas vapors ($k \approx 6$). Additionally, the effect of hydrocarbon vapor on the geoeletrical response may be to decrease the conductivity slightly, to the extent that these vapors tend to exclude or drive out soil moisture in the vadose zone directly above the free or residual product, Zone 3 of Sauck (2000) in Table 1.

The GPR sections show also several strong reflectors immediately bellow the GPR shadow zone (Figs. 4 and 5). Two strong reflectors seen in the data at approximately 2.3 and 2.5 m, which are respectively the depths to the capillary fringe and water table at the site, are of particular interest. Once more, the LNAPL could be displaced by water from the transition zone above the capillary fringe, thus making a sharp interface at the top of the water-saturated zone. Such a mechanism is suggested by Campbell et al. (1996) to explain an enhanced saturated zone reflection under a controlled spill experiment. Carcione et al. (2000) present a GPR modeling study in a contaminated air base in Poland. The radar simulation is based on a forward-modeling code and the synthetic radargrams show an enhancement water-table reflection, when a contaminated layer above the saturated zone is incorporated in the model above the saturated zone. The fact that the water table reflection is laterally discon-

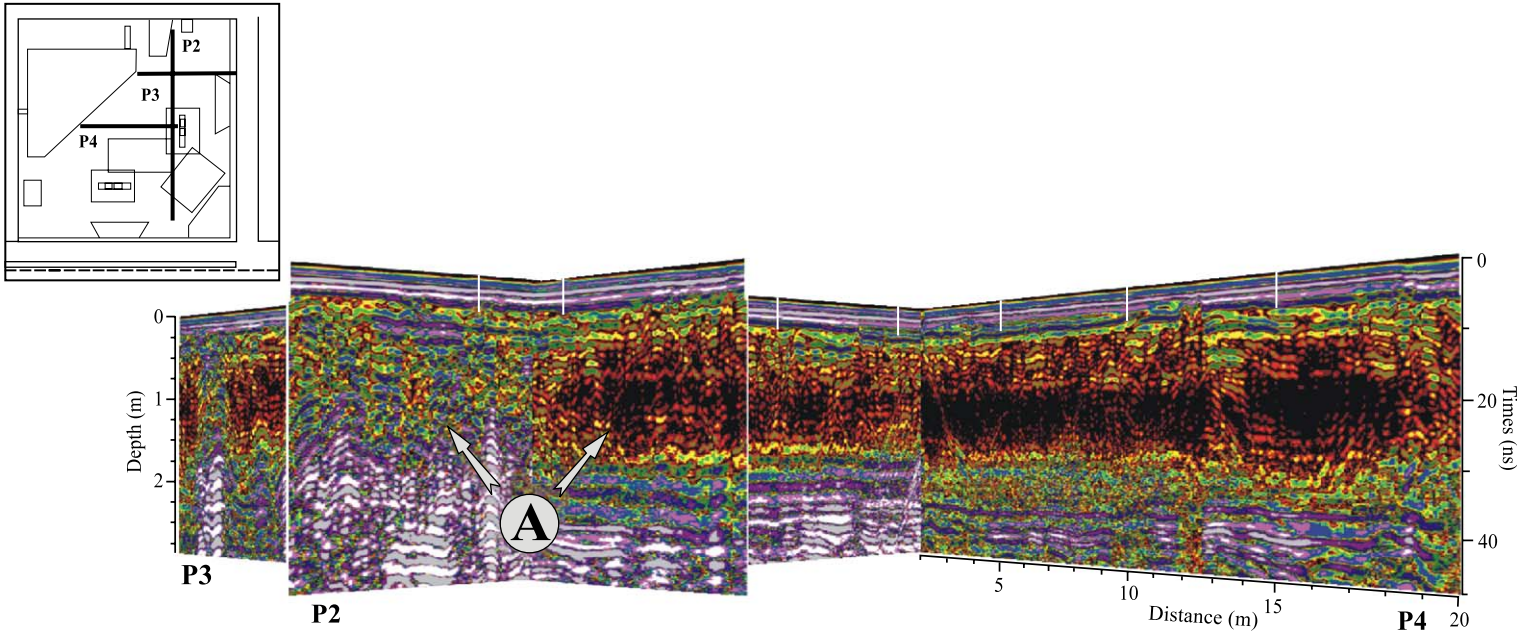

Fig. 5. The fence diagram obtained from profiles P2, P3 and P4 shows a prominent lateral variation in the radar sections (A), indicating the contaminant plume in the vadose zone. High reflectivity zones suggest more concentration of free/residual LNAPL products. Antenna frequency is centered in 400 MHz.

tinuous and varies its amplitude along the radar sections could be related to variable hydrocarbon concentrations directly above the water table.

There is a high reflectivity zone bellow the water table at 2.46 m (Figs. 4 and 5), which is possibly sandy soil saturated in a mixture of water and LNAPL products. The fact that contaminated groundwater samples were collected in the monitoring wells distributed on the gas station (Fig. 3) suggests that the presence of free and dissolved phases in the water does not attenuate GPR reflections at this study site. On the other hand, the reflections are apparently enhanced into the contaminated plume, but it is not so clear in the 200 MHz GPR data. At depth, this high reflectivity zone is apparently extended to 6.8 m (Fig. 4D), whereas there are lower amplitudes in uncontaminated areas in the NW border of the profile. Furthermore, the location of the new tanks is represented by a low reflectivity area, easily identified by a sharp break up of radar reflections, from 23 m to the profile end. The tops of the tanks can be observed by typical hyperbolic anomalies up to 1.0 m deep.

The GPR response for the 80 MHz antennas is shown in Fig. 4D. Several reflectors dominate the near surface radar section as far as 7.24 m deep. Both lower resolution and constructive and destructive interference of the electromagnetic waves at a shallow depth render seemingly impossible to detect the contaminant plume into the vadose zone. Even the water-table reflection is not easily identified on this radar section. The high reflectivity zone observed in the middle of the profile suggests the presence of gasoline free and/or dissolved in groundwater that is supported by hydrochemical analysis and higher frequency GPR data. Therefore, GPR data with 80 MHz antennas appear to be inapt to detect the hydrocarbon contamination in the vadose zone at the study site. However, this fact does not disqualify the use of lower frequencies antennas in contaminated areas because the GPR signal of organic contamination is highly site dependent.

6. Theoretical model for the plume

A simple geologic model is proposed to better understand and physically characterize the LNAPL behavior in the UST leakage site. The plume model is based on GPR field data and experimental and theoretical results described in the literature (e.g., Daniels et al., 1995; Campbell et al., 1996; Carcione and Seriani, 2000; Sauck, 2000). Additionally, a synthetic radargram will be present to evaluate the GPR response of the model in comparison with real data.

The plume model that simulates the LNAPL distribution at the underground in two different temporal phases is shown on Fig. 6. This model was adapted from Schwille (1988) and Guiger (2000) to a leaking fall, where the UST was partially located in the saturated zone in an initial phase (Fig. 6A). In a later scenario (Fig. 6B), the leaking tank has been removed and the water level suffered a strong draw down after the active pumping of groundwater took place.

In the studied case, the Zone 1 of Sauck (2000), as described in Table 1, are not present in the site due to the leakage occurred beneath the water table. Free and residual products compose the Zone 2, which tends to extend downwards, following the water level drop by continuous groundwater pumping. The vertical undergoing of free and residual products smear over that falling water table, forming a few meters of thickness geochemical zone saturated in hydrocarbon intermingled with water and air. According Sauck (2000), the residual phase may cause a horizon of decreased hydraulic conductivity, thus causing an increase in water content immediately above, whose upper boundary appears as reflectors in GPR sections, as pointed out by Campbell et al. (1996) in controlled spill experiments. Such signature can be easily identified in GPR data from Figs. 4 and 5.

The Zone 3 (Table 1) occurs directly above the free/residual product in the vadose zone (A in Fig. 6). This zone is subjected to varying amounts of rising hydrocarbon vapors, stemming in part from the simple devolatilization of the original LNAPL. In the radar sections, this zone is easily identified by the characteristic GPR shadow zone, caused by lower permittivity of the gas vapor relative to water, as it is the case in Figs. 4 and 5. Furthermore, the zones 4–6 have not been observed due to appear to be a minor contributor to geophysically detectable effects.

The synthetic radargram was computed using the forward-modeling code developed by Teixeira et al.

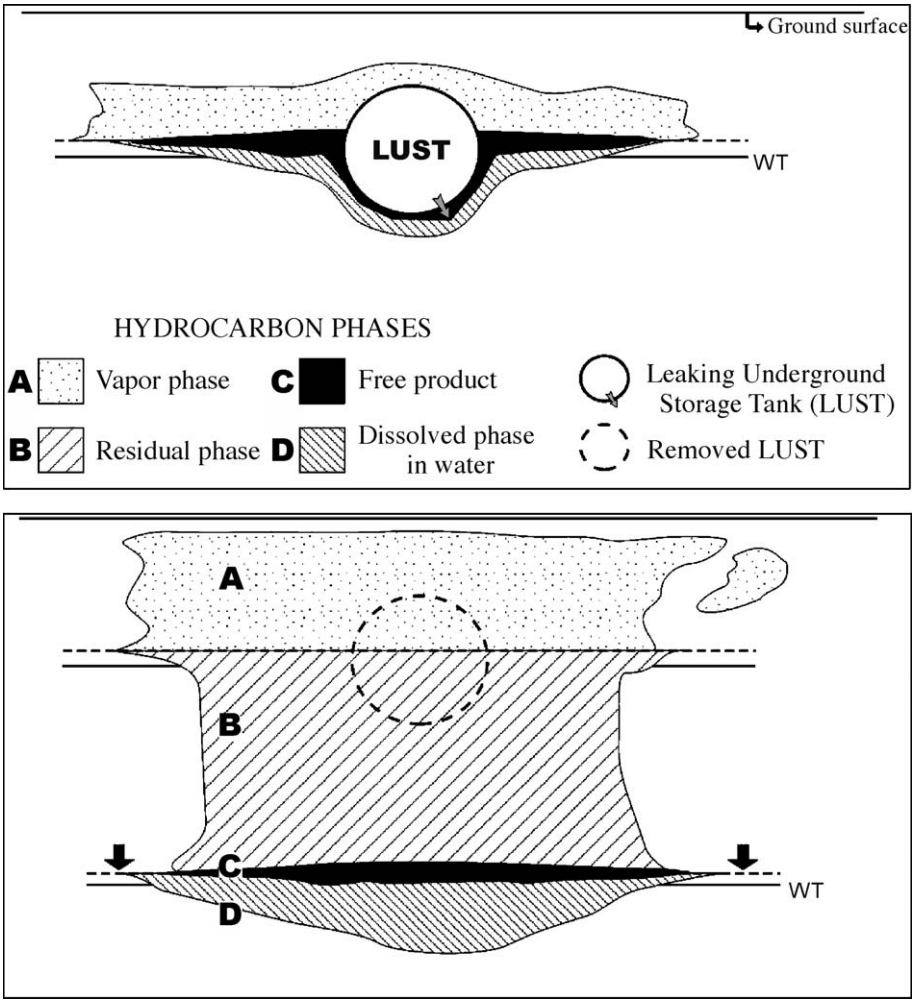

Fig. 6. Contaminant plume evolution by a falling water table condition. Model adapted from Schwille (1988) and Guiger (2000).

(1998). The modeling is based on a finite difference time domain (FDTD) numerical scheme for simulation of GPR on dispersive and inhomogeneous media with conductive loss. The soil dispersion is modeled by multiterm Lorentz or Debye models and incorporated into the FDTD scheme. The perfectly matched layer is extended to match dispersive media and used as an absorbing boundary condition to simulate an open space.

Fig. 7A summarizes parameters used in the GPR modeling that were defined in line with hydrogeological data obtained in monitoring wells and directly in the cave of the olds tanks, as well as based on prior information from the literature. The model consists of two soil layers, composed of 0.5 m thick of fine sand and 4.0 m thick medium aeolian sand, respectively. The lower unit is divided in three layers based on it fluid content (vadose, capillary fringe and saturated zones). The depths of capillary fringe and water table were taken as 2.3 and 2.7 m, in accordance with data from monitoring well MW01 (Fig. 3), obtained in May 2001. Ten months later, the water table was dropping to 5.17 m. In the contaminated zone, LNAPL products are incorporated in the fluid content together with water and air, providing a four-layer model (see Fig. 6).

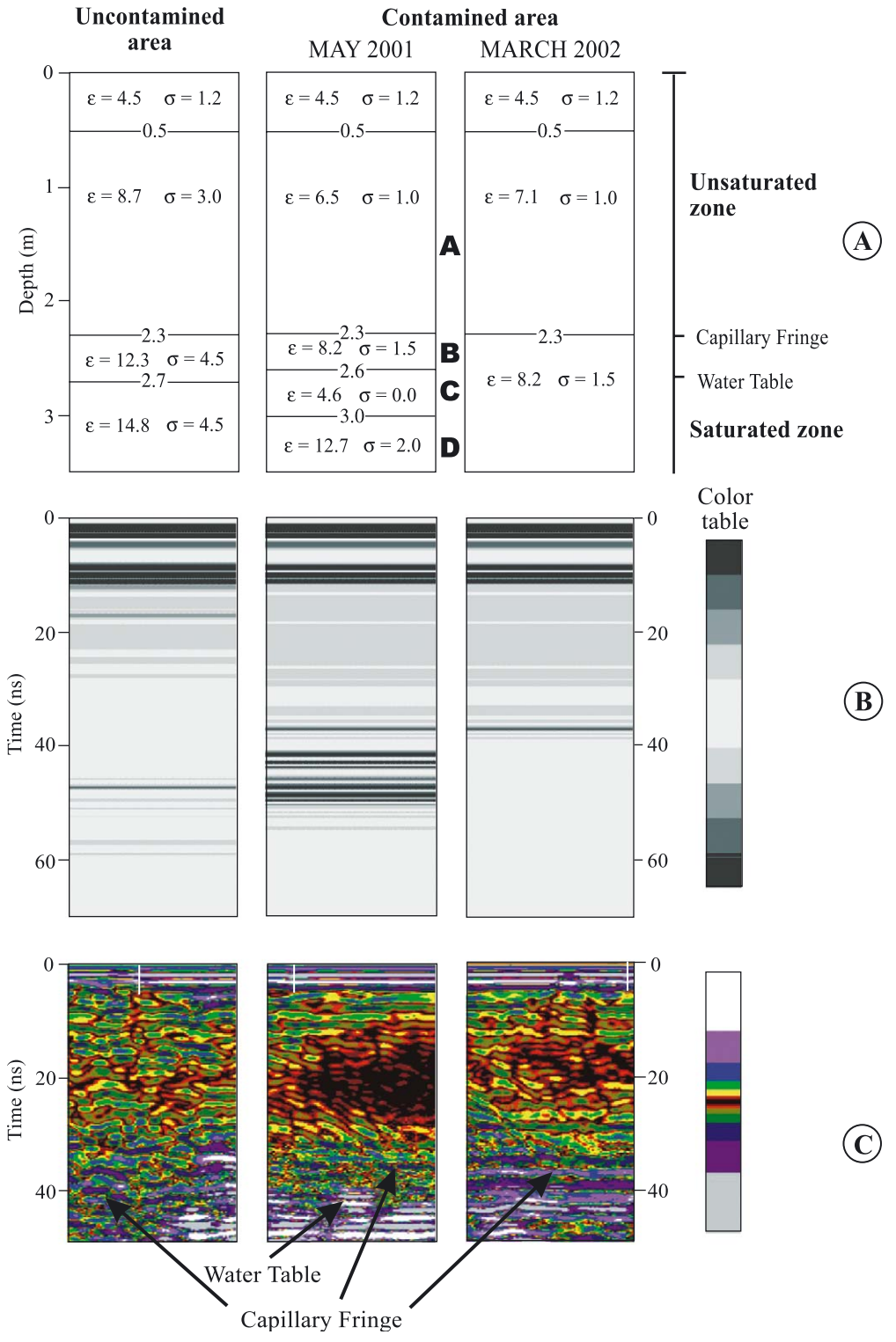
Uncontamined area
Contamined area
MAY 2001
MARCH 2002
Depth (m)
ε = 4.5 σ = 1.2
0.5
ε = 8.7 σ = 3.0
ε = 6.5 σ = 1.0
ε = 7.1 σ = 1.0
2.3
ε = 12.3 σ = 4.5
ε = 8.2 σ = 1.5
2.6
ε = 4.6 σ = 0.0
3.0
ε = 14.8 σ = 4.5
ε = 12.7 σ = 2.0
A
B
C
D
Unsaturated zone
Capillary Fringe
Water Table
Saturated zone
Color table
Time (ns)
Water Table
Capillary Fringe

Table 3
Precipitation records and depths of water table in the monitoring well MW01 obtained from January 2001 to March 2002

Year	2001												2002		
Month	JAN	FEB	MAR	APR	MAY	JUN	JUL	AUG	SEP	OCT	NOV	DEC	JAN	FEB	MAR
Rainfall (mm)	110.9	47.6	194.0	817.5	61.8	188.9	77.2	0.0	0.0	0.0	14.0	42.6	273.1	68.8	231.8
Water level (m)	2.35	2.36	2.35	2.32	2.67	2.82	3.37	3.79	4.03	4.43	4.75	4.93	4.97	5.12	5.17

In the lower soil unit, only variations in the fluids and not in porosity and lithology were considered. The permittivity of each layer was calculated by the empirical formula of Feng and Sem (1985), which considers water, air and hydrocarbon as individual inclusions. The dielectric constants used were 80 for water, 1 for air and 2 for LNAPL. The dielectric constant of the matrix was taken to be 7 because of the low clay content of the soil. Sediment porosity and conductivities, estimated from samplings, were taken as 20% and between 0.0 and 4.5 μS/m, respectively (Fig. 7A).

The synthetic radargram of both uncontaminated and contaminated areas for a 400 MHz antenna can be seen in Fig. 7B. The GPR signature of the area between vadose and saturated zones is very peculiar. In the uncontaminated area (synthetic radargram on left), the reflectors at 47 and 57 ns traveltime correspond to capillary fringe and water table, respectively. These reflections have lesser amplitude than in the contaminated area because the lower permittivity contrast. They represent a time delay up to 10 ns due to decrease of the propagation velocity in a more permissive medium. A section of profile P2 obtained with 400 MHz antennas can be seen in Fig. 7C (on the left), which shows a typical GPR signal of the uncontaminated area in the study site. The capillary fringe reflection occurs at 40 ns traveltime, whereas the reflection from the water table is located up to 55 ns. However, it is not reached in this profile.

In the middle synthetic radargram (Fig. 7B), the high reflective zone represents the GPR response to free, residual and dissolved phases, as described in Fig. 6. The GPR section of profile P2 (middle of Fig. 7C) illustrates the condition of the impacted area in May 2001. The low reflectivity zone in the upper part of the section correspond to the vadose zone contaminated by vapor product, whereas after 35 ns traveltime the reflections became more pronounced in response to presence of LNAPL phases. This GPR signature is consistent with the synthetic radargram (middle of Fig. 7B) and strongly supported by previous resulted discussed in the literature (Daniels et al., 1995; Campbell et al., 1996).

On the right of Fig. 7B, there is a falling water table condition, where the lower layer corresponds to a contaminated area for residual product (B in Fig. 6). In the GPR data of profile P2 collected in March 2002 (right of Fig. 7C), the capillary fringe reflection is located at 37 ns traveltime, marking the upper limit of the residual phase zone. The decrease of the reflections amplitude suggests a lower concentration of LNAPL due to their downwards migration, following the water table drop during the corrective action. The reduction of the shadow zone is consistent with a concomitant decrease of the vapor product concentration in the vadose zone.

7. Evolution of the plume

Since May 2001 the groundwater has regularly been pumped to reduce the contamination. The extracted LNAPL and water was treated properly and disposed in the city sewage system. The treated water was not pumped back to the ground. This corrective action was directly responsible for a strong water table drop up to 3.5 m at the study site since May 2001. Both rainfall records and water depths in the monitoring well 01 (MW01) are show in Table 3. The highest rainfall occurred from January to July 2001. The other months of the year represented the

Fig. 7. (A) Geometries and physical parameters of the model. (B) Synthetic radargrams for a 400 MHz antenna based on the forward modeling code developed by Teixeira et al. (1998). (C) GPR sections of profile P2 collected on uncontaminated area (on the left), and on contaminated area: in May 2001 (on the middle) and in March 2002 (on the right). ε: constant dielectric. σ: conductivity in μS/m.

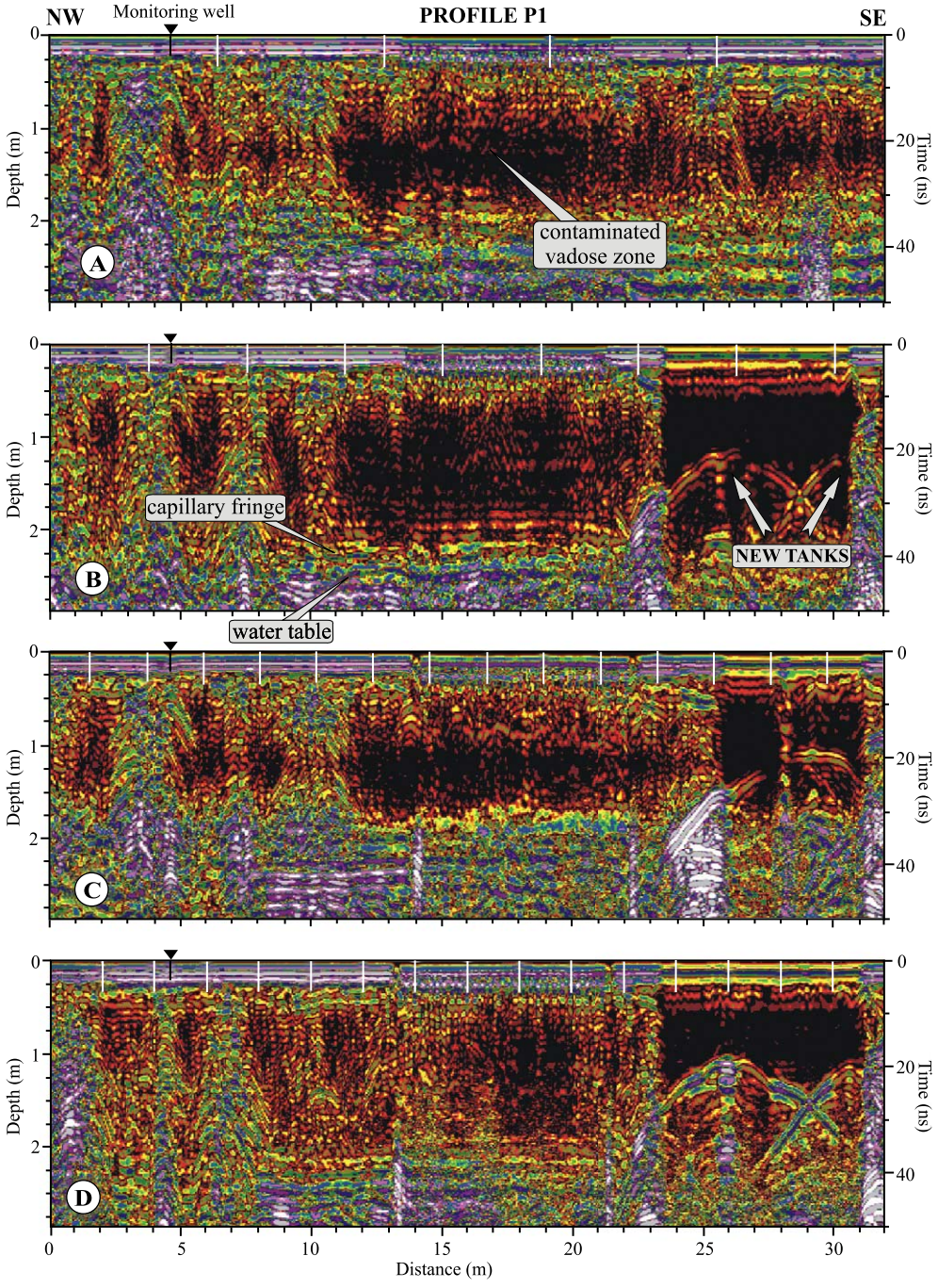

Fig. 8. GPR sections at profile P1 show changes in the electromagnetic signal during the remediation process. Antenna frequency is centered in 400 MHz. (A) January 2001, (B) May 2001, (C) September 2001, and (D) March 2002.Vertical scale exaggeration = 3.5.

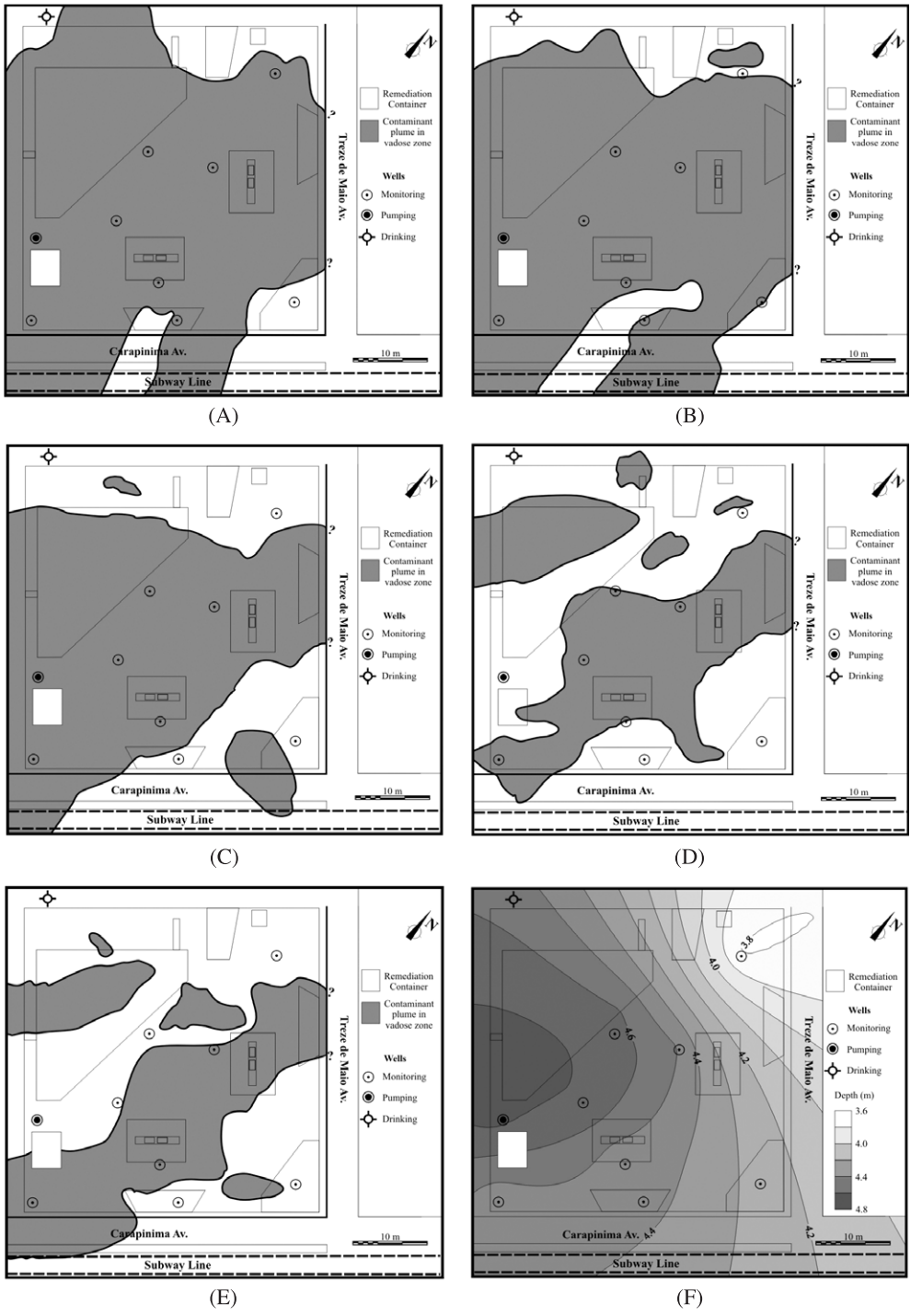

Fig. 9. Evolution of the plume in the vadose zone during the corrective action (A–E). November water table map (F), showing a NNE–SSW oriented groundwater flow.

dry season at the whole region. But the water level remained constant until May, when the remediation process begun effectively. Hence, the water table drop strongly induced by pumping wells reduced the dependency on seasonal changes that occurred in the study site.

Groundwater samples were collected from monitoring wells between January 2001 and March 2002. Ceará State Environmental Agency (SEMACE) analysed them for total petroleum hydrocarbon (TPH) using an infrared chromatograph. Water analyses indicate that the amount of TPH decreases slowly but continuously along this time window. Therefore, the study site still remains impacted from the hydrochemical point of view during the GPR survey, despite of the decrease of the LNAPL concentration.

In a water-table drop scenario, significant changes in the GPR response of the contaminated area are expected. Indeed, an overall increase in the signal amplitudes could be observed in sections obtained at profile P1 at different times (Fig. 8), mainly in the vadose zone. This reflectivity enhancement corresponds probably to lower concentrations of the vapor phase above the falling water table. The LNAPL compounds respond to changes in water saturation and promote a vertical displacement (Steffy, 1997). In fact, the top of the low reflectivity zone became slightly deeper along the remediation process (Fig. 8). Nevertheless, the horizontal reduction of the plume was much more pronounced.

The GPR responses to falling water table (Fig. 8) could be better understood on the basis of the plume evolution model from Fig. 6. During water level drop, the two strong reflectors up on 2.46 m are not more directly associated with the water table, but probably with the interface between vapor and residual hydrocarbon phases. The upper contaminated zone (A in Fig. 6B) represents a mixture of vapor phase and air with relative lower moisture content, whereas the residual zone (B in Fig. 6B) should contain higher LNAPL concentration in detriment of air and water content. A permittivity contrast between these couple media appears to be significant enough to guarantee high amplitude reflections (see synthetic radargrams in Fig. 7). This high reflectivity transition zone reached a thickness of 2.7 m in March 2002, when the water table dropped to 5.17 m (Table 3). During a water-table drop, both free and dissolved products, which were once partially immobilized in the saturated zone migrate vertically, smeared slowly the contaminant residual phase within the transition zone (Steffy, 1997), the Zone 2 of the plume model of Sauck (2000) in Table 1.

The spatial distribution of the contaminant plume by several GPR surveys is shown in Fig. 9. In January 2001, most of the ground bellow the gas station was impacted by LNAPL vapor phase (Fig. 9A), whereas 15 months later the contaminated plume was restricted to a narrow N–S oriented belt in the middle of the site, as well as several isolated hydrocarbon poolings (Fig. 9E). This orientation coincided with the groundwater gradient, identified by water level measurements from monitoring wells (Fig. 9F). The N–S oriented groundwater flow followed the local topographic gradient and was artificially accentuated by active pumping at the south end of the gas station. In any way, the vapor phase had a tendency to be concentrated where the water table formed more expressive depressions. This occurred in response to new hydrostatic conditions in the subsurface at the study site. Unfortunately, the plume at Treze de Maio Avenue was difficult to detect due to an underground gallery. It runs parallel to the street, close to sidewalk, and has a very thick concrete layer at the top. The LNAPL compounds probably migrate bellow this structure, whose base is located up to 3 m deep.

Another interesting aspect about the plume evolution in the unsaturated zone is presented on Fig. 9. It is the occurrence of hydrocarbon pooling as soon as the contaminated zone was reduced. Lateral heterogeneities of hydrogeologic parameters determine a non-uniform LNAPL migration in the vadose zone (Domenico and Schwartz, 1990; Daniels et al., 1995), which was probably what occurred in the study area. During the GPR monitoring, the hydrocarbon poolings change relatively fast in their dimensions and locations, following approximately the groundwater flow.

8. Conclusions

A 4-D GPR survey was carried out to detect and monitor a contaminant plume produced by gasoline leaking from an underground storage tank. GPR data were collected during a corrective action put into

effect to reduce the contamination along fifteen months. Groundwater analysis in strategically located wells gave support to outline the impacted area undergrounds. Finally, forward modeling gave theoretical support to understand the GPR signal of the polluted site.

Different radar frequencies were used to characterize the GPR signature of the LNAPL plume. GPR data at 400 and 200 MHz provided the best compromise between resolution and penetration depth at the study site. In GPR sections, the presence of LNAPL in the vadose zone was easily detectable by a zone of strong diminished reflections. The low permittivity of hydrocarbon product relative to water caused attenuation of GPR signal in near the surface. On the other hand, radar measurements showed enhanced reflections in contaminated transition and saturated zones. The water table reflection had higher amplitudes, where poolings of gaseous LNAPL displaced the water from transition zone above the capillary fringe. Further, the saturated zone apparently became more reflectivity due to hydrocarbon dissolved in water. Synthetic radargram based on geoelectric models appears to explain well these different GPR responses corresponding to LNAPL geochemical zones.

A successfully detection of the plume was facilitated by geologic and hydrogeologic conditions in the study site. The permittivity contrast between LNAPL, air, and water was normally high in a sandy soil with low clay content. A shallow water table and an expressive lateral variation of the GPR signal allowed characterizing the contaminant plume at the gas station. However, GPR response over hydrocarbon spills is both site and time dependent. This can lead to ambiguous interpretation when a clear shadow zone is not easily identified and information on subsurface conditions from soil and water probes is unavailable. Furthermore, the presence of 24% ethanol in the Brazilian gasoline played no important role in the detection of the contaminant plume probably due to the relative permittivity of both organic compounds ranging from 6 to 7 at the GPR signal frequency.

During the remediation process, a pumping well was used to pump free product and contaminated water. The more significant hydrogeologic change in this case was a strong water table drop at the study site. The water-table drop smeared residual hydrocarbon phase within the transition zone. This could be observed in GPR sections and is supported by monitoring wells data. Radar measurements revealed also an increase of signal amplitude within the low reflectivity zone. In the case of a deeper water table, the strong reflection, which initially marked the water table, apparently represents now an interface between upper vapor phase and lower residual phase of LNAPL. This may be a consequence of a decrease on gaseous hydrocarbon concentration due to diminished water pressure. In fact, the spatial evolution of the plume in vadose zone followed groundwater flow during the pumping process. This suggests that the LNAPL vapor phase has a tendency to migrate to sites where the water pressure is weaker.

Acknowledgements

The authors acknowledge the financial support from the CTPETRO/CNPq (No. 465569/00-5), PADCT III (No. 620154/97-7) and CTPETRO/FINEP/CNPq (No. 22010739/00-1277/01) programs. The Ceará State Environmental Agency (SEMACE) provided hydrochemical analysis. The oil company that permitted the research inside the gas station plant. The company in charge of the remediation procedure provided technical data about water pumping action. Our appreciation is extended to F.L. Teixeira (Department of Electrical Engineering-Ohio State University) for the GPR forward-modeling code and suggestions on the manuscript. The authors also gratefully acknowledge to Dr. F.H.R. Bezerra and Dr. L. Bianchi for assistance in text review.

References

Asquith, G.B., Gibson, C.R., 1982. Basic well log analysis for geologists. AAPG. 216 pp.

Benson, A.K., Payne, K.L., Stubben, M.A., 1997. Mapping groundwater contamination using dc resistivity and VLF geophysical methods—a case study. Geophysics 64 (1), 80–86.

Brandão, F.L., 1995. Projeto SINFOR: Mapa geológico da região metropolitana de Fortaleza. Texto Explicativo. Série Cartas Temáticas. 34 pp.

Campbell, D.L., Lucius, J.E., Ellefsen, K.J., Deszcz-Pan, M., 1996. Monitoring of a controlled LNAPL spill using ground penetrating radar. Proceedings of the Symposium Application of Geophysics to Engineering and Environmental Problems (SAGEEP'96). Keystone, CO, USA, pp. 511–517.

Carcione, J.M., Seriani, G., 2000. An electromagnetic modelling tool for the detection of hydrocarbons in the subsoil. Geophysical Prospecting 48 (2), 231–256.

Carcione, J.M., Marcak, H., Seriani, G., Padoan, G., 2000. GPR modeling study in a contaminated area of Krzywa air base (Poland). Geophysics 65 (2), 521–525.

Corseuil, H.X., Fernandes, M., Rosário, M., Seabra, P.N., 2000. Results of a natural attenuation field experiment for an ethanol-blended gasoline spill. Proceedings of the 2000 petroleum hydrocarbon and organic chemicals in ground water. Anaheim, CA, USA, pp. 24–31.

Daniels, J.J., Roberts, R., Vendl, M., 1992. Site studies of ground penetrating radar for monitoring petroleum product contaminants. Proceedings of the symposium application of geophysics to engineering and environmental problems (SAGEEP'96), vol. 2. Oak Brook, IL, USA, pp. 597–609.

Daniels, J.J., Roberts, R., Vendl, M., 1995. Ground penetrating radar for the detection of liquid contaminants. Journal of Applied Geophysics 33, 195–207.

Davis, J.L., Annan, A.P., 1989. Ground-penetrating radar for high-resolution mapping of soil and rock stratigraphy. Geophysical Prospecting 37, 531–551.

Domenico, P.A., Schwartz, F.W., 1990. Physical and Chemical Hydrogeology Wiley, New York. 824 pp.

Feng, S., Sem, P.N., 1985. Geometrical model of conductive and dielectric properties of partially saturated rocks. Journal of Applied Physics 58, 3236–3242.

Guiger, N., 2000. Poluição de águas subterrâneas e do solo causada por vazamentos em postos de abastecimento. Waterloo Hydrogeologic, Ontario. 356 pp.

Olhoeft, G.R., 1986. Direct detection of hydrocarbon and organic chemicals with ground penetrating radar and complex resistivity. Proc. NWWA/API Conference Petroleum Hydrocarbons and Organic Chemicals in Ground Water–Prevention, Detection and Restoration. National Water Well Association, Dublin, pp. 284–305.

Redman, J.D., Deryck, S.M., Annan, A.P., 1994. Detection of LNAPL pools with GPR: theoretical modeling and surveys of a controlled spill. Proceedings of the Fifth International Conference on Ground Penetrating Radar (GPR'94), Kitchener, Ontario, Canada, Expanded Abstract, pp. 1283–1294.

Sauck, W.A., 2000. A model for the resistivity structure of LNAPL plumes and their environs in sandy sediments. Journal of Applied Geophysics 44, 151–165.

Schwille, F., 1988. Dense Chlorinated Solvents in Porous and Fractured Media. Lewis Publishers, Chelsea. 146 pp.

Steffy, D.A., 1997, Vertical immiscible displacement and entrapment of an LNAPL by a fluctuating water table—a field, laboratory and numerical study. PhD Thesis, University of Western Australia, Reference ED 681 DS. 172 pp.

Teixeira, F.L., Chew, W.C., Straka, M., Oristaglio, M.L., Wang, T., 1998. Finite-difference time-domain simulation of ground penetrating radar on dispersive, inhomogeneous, and conductive soils. IEEE Transactions on Geoscience and Remote Sensing 36 (6), 1928–1937.